Computer simulations of disordering kinetics in irradiated intermetallic compounds

M. Spaczér
Ecole Polytechnique Fédérale de Lausanne–CRPP, Fusion Technology Division, CH-5232 Villigen PSI, Switzerland

A. Caro
Ecole Polytechnique Fédérale de Lausanne–CRPP, Fusion Technology Division, CH-5232 Villigen PSI, Switzerland and Centro Atómico Bariloche, 8400 Bariloche, Argentina

M. Victoria
Ecole Polytechnique Fédérale de Lausanne–CRPP, Fusion Technology Division, CH-5232 Villigen PSI, Switzerland

T. Diaz de la Rubia
Lawrence Livermore National Laboratory, Livermore, California 94550
(Received 4 February 1994)

Molecular-dynamics computer simulations of collision cascades in intermetallic Cu_3Au, Ni_3Al, and NiAl have been performed to study the nature of the disordering processes in the collision cascade. The choice of these systems was suggested by the quite accurate description of the thermodynamic properties obtained using embedded-atom-type potentials. Since melting occurs in the core of the cascades, interesting effects appear as a result of the superposition of the loss (and subsequent recovery) of the crystalline order and the evolution of the chemical order, both processes being developed on different time scales. In our previous simulations on Ni_3Al and Cu_3Au [T. Diaz de la Rubia, A. Caro, and M. Spaczér, Phys. Rev. B **47**, 11 483 (1993)] we found a significant difference between the time evolution of the chemical short-range order (SRO) and the crystalline order in the cascade core for both alloys, namely the complete loss of the crystalline structure but only partial chemical disordering. Recent computer simulations in NiAl show the same phenomena. To understand these features we study the liquid phase of these three alloys and present simulation results concerning the dynamical melting of small samples, examining the atomic mobility, the relaxation time, and the saturation value of the chemical short-range order. An analytic model for the time evolution of the SRO is given.

I. INTRODUCTION

It is well established that irradiation of ordered intermetallic compounds may induce disordering or amorphization depending on the projectile characteristics, irradiation conditions, and composition of the target. Electron, self-ion, and light-ion irradiations of Cu_3Au at low temperatures induce disorder. In the Ni-Al system, electron irradiation at low temperatures completely disorders Ni_3Al, and partially disorders NiAl.[1] However, at the same temperature, heavy-ion irradiation induced amorphization both in Ni_3Al and NiAl,[2–6] while light-ion irradiation will only produce partial amorphization or partial chemical disordering.

To give a microscopic view of these features, we reported in previous publications[7,8] molecular dynamics computer simulations applied to two intermetallic compounds, namely, Ni_3Al and Cu_3Au, studying the displacement cascades created by energetic recoils. These two compounds were chosen because (i) they have the same crystalline structure ($L1_2$) but different order-disorder behavior (Cu_3Au has an order-disorder transition at $0.55T_m$, while Ni_3Al remains ordered up to the melting point), (ii) embedded atom potentials work very well for the constituent species and can also reproduce the main features of the phase diagrams, (iii) as indicated above, extended irradiation experimental results are available.

The previous simulations showed a significant difference between the evolution of the short-range order (SRO) and the crystalline order parameters in both $L1_2$ intermetallics: a complete loss of the crystalline structure, and only a partial chemical disorder in the core of the cascade. Recent simulations with 5-keV Ni primary knock-out atoms (PKA) in NiAl ($B2$ structure) result in a very similar behavior of these two parameters compared with the $L1_2$ structures. The minimum value of the short-range order parameter in the cascade core reached during the lifetime of the heat spike is about 0.53 in NiAl (the corresponding values are 0.68 and 0.48 in Ni_3Al and Cu_3Au, respectively) and the crystalline order parameter reaches zero at 0.2 psec after the cascade starts.

II. SIMULATION METHODS

Extended computer simulations are employed to determine the equilibrium thermodynamic and static point defect properties of the three alloys as well as the time evolution of the order parameters during the dynamical melting. These include molecular dynamics and Monte Carlo techniques.

The cascade simulations were performed in lattices containing a large number of atoms (157 216 for the $L1_2$ alloys and 109 744 for NiAl) with periodic boundaries at constant volume. Small lattices (256, 864, or 2048 atoms for the $L1_2$ alloys and 432 or 1024 atoms for NiAl) with 5% randomly distributed vacancies were created for the dynamical melting calculations. The constant stress method of Parrinello and Rahman[9,10] was used for controlling the motion of the periodic boundaries. For the static point-defect properties and Monte Carlo calculations the same small samples were used but without vacancies. The reasons to introduce 5% vacancies are that (i) without vacancies an infinite perfect lattice would be simulated, which is unrealistic from the viewpoint of the melting temperature and (ii) the amount of vacancies used represents the change in volume under melting.

The embedded atom potentials reported in Refs. 11 and 12 reproduce fairly well the equilibrium thermodynamic properties, i.e., cohesive energy, lattice constant, bulk modulus of the Cu-Au and Ni-Al systems, and the most important features of the phase diagram. It has also been shown that the embedded atom method (EAM) can describe the liquid phase of some transition metals such as Ni, Cu, and Au in good agreement with the experimental data.[13] Monte Carlo simulations with very small samples (256 and 432 atoms for the $L1_2$ and $B2$ structures, respectively) with up to 1 000 000 steps result in an order-disorder transition in Cu_3Au at around 330±40 K, and melting at 1410±60 K (experimental values are 663 and 1213 K). For Ni_3Al the corresponding temperatures are ~1290±50 K and 1790±50 K (experiments give 1668 K for both). The NiAl lattice melts in the ordered phase at 1600±40 K (measured value is 1911 K). Short-time molecular-dynamics simulations cannot predict the order-disorder transition and result in values of the melting temperatures of the ordered phases at ~1670±40, 1100±70 and 1600±30 K in Ni_3Al, Cu_3Au and NiAl, respectively. The aim of this work is to give a microscopic explanation of the behavior of the chemical short-range order during the cascade quenching based on the liquid phase properties of these three alloys.

III. RESULTS AND DISCUSSION

A. Elementary point defect properties

The elementary point-defect properties of the two $L1_2$ intermetallics were already calculated in Refs. 7, 12, and 14, with the same type of EAM potentials used in this work for Cu_3Au and Ni_3Al, respectively, and in Ref. 15 with different EAM potentials for Ni_3Al. In this work we extend those studies to include also the NiAl case. In Table I we report some thermodynamic properties predicted by the EAM potentials, i.e., the heating of melting ($\Delta H_{\rm melt}$), heat of disordering ($\Delta H_{o\text{-}d}$), formation enthalpy of the ordered and disordered phases ($\Delta H_f^{\rm ordered}$ and $\Delta H_f^{\rm disordered}$), respectively, and summarize the formation enthalpies (in eV) and formation volumes (in Ω_0 in units, where Ω_0 is the volume per atom in a 0-K equilibrium lattice) of vacancies, antisites and several interstitial configurations. The disordered state of the alloys was created with random occupation of the lattice sites by the different types of atoms in such a way that the composition of the sample was preserved. Three different random configurations were averaged for all of the examined intermetallics. The definition of the defect formation energy used by us is the following:

$$E_f^{\rm defect}=\frac{N}{N\pm1}E(N\pm1,\text{defect})-E_0(N)\ , \tag{1}$$

where $E(N\pm1,\text{defect})$ is the energy of the system of N lattice sites containing $N\pm1$ atoms and the defect [here the (+) sign stands for interstitials and the (−) sign for vacancies]. $E_0(N)$ denotes the energy of the equilibrated perfect crystal containing N atoms. The choice of a reference state in the case of alloy calculations is not well defined.[15] The choice made in our definition Eq. (1) is further justified in the discussion that follows. The definition of the defect formation energy for vacancies in binary alloys according to Refs. 12 and 15 is

$$E_f^{v_A}=\Delta E^{v_A}+\mu_A\ , \tag{2}$$

where ΔE^{v_A} is the difference in energy between the ideal lattice and the lattice with one vacancy on the A sublattice (defect energy) and μ_A is the chemical potential for type-A atoms.

Our molecular dynamics simulations on the static point defect properties were performed at fixed number of atoms and temperature, while the pressure was controlled by the Parrinello-Rahman method.[9,10] This implies an isothermal-isobaric ensemble where the chemical potential μ_A is

$$\mu_A=\left.\frac{\partial G}{\partial N_A}\right|_{T,p,N_B}\ . \tag{3}$$

Because of the definition of the defect energy (ΔE^{v_A}), it is clear that

$$\Delta E^{v_A}=E(N-1,v_A)-E_0\ .$$

Comparing Eq. (1) with Eq. (2), it is easy to see that the chemical potential of the type-A atoms (μ_A) corresponds to $E(N-1,v_A)/(N-1)$ in our calculation. At zero temperature and pressure the internal energy of the system is equal to the Gibbs free energy ($G=E-TS+pV$) regardless of small fluctuations. By using the correspondence

$$\mu_A\mapsto\frac{E(N-1,v_A)}{N-1}\ ,$$

we have made nothing else than approximate a derivative given by Eq. (3) by the difference in the range of $[0,N-1]$. This approximation is precise if the variation of the internal energy with the number of atoms is not far from linear at zero temperature and pressure and also if the fluctuations in the energy are small. We assumed that in our simulated system these conditions are valid. In order to verify these assumptions we have compared our simulation results performed in three different sizes of samples (256, 864, and 6912 atoms) with the calcula-

tion presented in Ref. [12] on Ni_3Al, where the vacancy formation energies were calculated with a grand-canonical ensemble and the formation energies were given by Eq. (2). The defect energies for the Ni vacancy are 6.096, 6.104, 6.100, and 6.10 for $N=6912$, 864, 256 atoms, and in Ref. 12, respectively. The formation energies of a Ni vacancy are 1.468, 1.477, 1.476, and 1.47, respectively. The agreement for the defect energy and the formation energy of the Al vacancy is also very good. The formation volumes were calculated on the same way.

According to Table I we find a considerable difference between the antisite formation energies in the Cu-Au and Ni-Al systems (0.026 eV/atom in Cu_3Au, 1.30 and 2.26 eV/atom in Ni_3Al and NiAl, respectively). We also observe the following interesting behavior in the energetics of the several self-interstitials that may exist in these structures. If we sort the interstitials by increasing formation enthalpy, we observe one of these two alternatives: (i) the chemical nature of the interstitial determines which are those energetically preferred to (ii) the location of the defect is more important than its type to determine the enthalpy. In Ni_3Al and Cu_3Au the interstitials with lowest formation enthalpy are always in the N-type layers (the layers which contain only Ni or Cu atoms), while in NiAl the defects with the lowest formation enthalpy are always Ni interstitials, regardless of the layer in which they are located. It also happens in Ni_3Al that at a given layer, the Ni interstitials have lower formation enthalpy than the Al ones. This is not the case in Cu_3Au, where in the M-type layer (M means mixed layer, which contains 50-50 % of the constituent, according to the notation of Ref. 15), the Cu interstitials have lower formation enthalpy, while in the N layer the sequence is just the opposite. This is one possible reason to explain the different disordering energies of these two alloys.

B. Dynamical melting simulations

We use molecular dynamics to follow the order parameters during a simulation of ultrafast melting of a small sample. A heat pulse is created by scaling the velocities at $t=0$ with several initial temperatures between 3500 and 14 000 K in the samples containing 5% vacancies with constant energy and mobile boundary conditions.

TABLE I. Some simulated thermodynamical data and the point-defect properties of Ni_3Al, Cu_3Au, and NiAl. Units are eV/atom. T^{sim} is the melting temperature given by the respective technique. $t1$ marks Ni atoms in the two Ni-Al systems and Cu atoms in Cu_3Au, while $t2$ stands for Al and Au atoms, respectively.

Defect properties		Caro *et al.*[a] Ni_3Al ΔE_f	Caro *et al.*[a] Ni_3Al ΔV_f	Bacon *et al.*[b] Ni_3Al ΔE_f	Bacon *et al.*[b] Ni_3Al ΔV_f	This work[c] Ni_3Al ΔE_f	This work[c] Ni_3Al ΔV_f	This work[c] Cu_3Au ΔE_f	This work[c] Cu_3Au ΔV_f	This work[d] NiAl ΔE_f	This work[d] NiAl ΔV_f
Vacancy	$t1$	1.47	0.96	1.42	0.87	1.47	1.14	0.82	0.63	1.64	1.80
Vacancy	$t2$	1.91	0.83	1.65	0.75	1.92	1.01	1.87	0.40	1.07	1.38
Antisite	$t1_{t2}$	0.54	0.35	0.31	−0.06	0.54	0	0.66	−0.43	−0.22	0.0
Antisite	$t2_{t1}$	0.58	0.35	1.02	0.31	0.58	0.06	−0.40	0.376	2.12	0.22
Antisite	Pair					1.30	0.0	0.26	0.0	2.26	0.0
Octahedral	$t1$ (N)	3.77	0.47	3.65	0.89	3.77	−0.67	1.32	0.046	4.70	−0.58
Octahedral	$t1$ (M)	4.97	1.11	5.11	1.20	4.98	−0.53	3.08	0.55	4.49	−0.60
Octahedral	$t2$ (N)	4.54	0.87	3.94	0.97	4.55	−0.51	1.03	0.524	6.92	−0.50
Octahedral	$t2$ (M)	6.53	1.53	e		6.53	−0.11	3.36	1.192	6.97	−0.46
Dumbell	$t1$-$t1^f$ (N)	3.63	0.67	3.55	0.67	3.62	0.84	1.23	0.039	4.49	0.32
Dumbell	$t1$-$t1^f$ (M)	4.67	0.85	4.80	0.65	4.67	1.16	2.83	0.49	No	No
Dumbell	$t2$-$t2^a$ (M)	6.22	1.38	5.92	1.44	6.20	1.72	3.22	1.127	6.93	−0.26
Dumbell	$t1$-$t2^f$ (N)	4.45	1.00	g		4.45	1.25	1.08	0.508	6.34	0.31
Dumbell	$t1$-$t2^f$ (M)	6.21	1.59	5.83	1.04	h		2.94	1.039	No	No
Dumbell	$t1^f$-$t2$ (M)	4.89	1.11	4.87	1.11	4.88	1.28	2.98	0.54	4.69	−0.66

Thermodynamic properties	Technique	Ni_3Al	Cu_3Au	NiAl
ΔH_{melt} at T^{sim}	Monte Carlo	0.169	0.089	0.222
ΔH_{melt} at T^{sim}	Molecular dynamics	0.152	0.053	0.153
$\Delta H_{o\text{-}d}$ at 0 K	Energy minimization	0.103	0.024	0.197
$\Delta H_f^{ordered}$ at 0 K	Energy minimization	−0.396	−0.051	−0.488
$\Delta H_f^{disordered}$ at 0 K	Energy minimization	−0.293	−0.027	−0.291

[a]5324 atoms.
[b]4000 atoms.
[c]864 atoms.
[d]1024 atoms.
[e]Convert to $t2$-$t2$ (M) dumbell.
[f]Extra atom.
[g]Convert to $t2$ (N) octahedral.
[h]Convert to $t1$-$t1$ (M) dumbell with $\Delta E_f=5.02$ eV and $\Delta V_f=1.61\ \Omega_0$.

The time averages calculated between 4 and 5 psec for the $L1_2$ alloys and between 2.5 and 3 psec for NiAl give the final values for the temperature, volume, and energy of the sample that undergoes a fast-melting transition and also give the saturation value (S_{sat}) of the short-range order parameter and the coordination number in the first-neighbor shell, while from the time evolution of these parameters we can determine the relation time (τ) of SRO. In Fig. 1 we plot the short-range order parameter [which will be defined in the next section by Eq. (5)], the crystalline order parameter (for a definition, see, e.g., Ref. 7), and the temperature as a function of time to show a typical response of these quantities to the heat pulse.

1. The temperature dependence of the saturation value of SRO

Changing the amount of energy in the heat pulse, we obtain different final temperatures, and we observe that the saturation value of the short-range order parameter depends on this final temperature. In a first approximation we assume an exponential dependence of the saturation value of SRO with the inverse of the temperature:

$$S_{sat}(T)=S_0\exp\left[\frac{\Delta H_{sat}}{kT}\right], \tag{4}$$

where the two parameters S_0 and ΔH_{sat} are determined from the simulations. Five events were performed in the two Ni-Al intermetallics, up to 3 and 5 psec in NiAl and Ni_3Al, respectively. In the case of Cu_3Au nine simulations were made in samples containing 824 atoms (seven events up to 5 psec and two up to 6 psec) and one event with 1948 atoms up to 5 psec.

The definition of the short-range order parameter used is

$$\gamma_{t2}^{SRO}=\frac{Z(t1|t2)-Z^{mix}(t1|t2)}{Z^{perf}(t1|t2)-Z^{mix}(t1|t2)} \tag{5}$$

for the minority species (Al or Au, noted further as $t2$ for type-2 atoms) and

$$\gamma_{t1}^{SRO}=\frac{Z(t2|t1)-Z^{mix}(t2|t1)}{Z^{perf}(t2|t1)-Z^{mix}(t2|t1)} \tag{6}$$

for the majority species (Ni and Cu, noted further as $t1$ for type-1 atoms).

In the above definitions $Z(t1|t2)$ and $Z(t2|t1)$ denote the number of unlike neighbors in the first coordination shell of the $t2$ and $t1$ atoms, respectively. The first coordination shell was defined as a sphere of radius equal to the average between the first- and second-nearest-neighbor distance in the crystalline phase. Z^{mix} and Z^{perf} have the same meaning but in the random alloy and in the perfectly ordered intermetallic, respectively. Using this definition the range of SRO is in the [0,1] interval, where 0 indicates an ideal random mixture. Figure 2 shows the temperature dependence of the average of SRO calculated from the corresponding values of the minority and majority species by weighting respect to their concentration (our model curves).

The short-range order parameter traditionally used in the literature of the binary liquid alloys is that known as Cowley-Warren, α_1, for the first-neighbor sphere. It is defined in terms of the conditional probability $[A/B]$, that is the probability that an atom A sits at site 2 as a nearest neighbor of a B atom at site 1, see, e.g.,[16]

$$[A/B]=c(1-\alpha_1)\ . \tag{7}$$

From the viewpoint of theoretical modeling, the binary molten alloys may be classified into two main categories, named symmetric and asymmetric alloys. Properties like the free energy of mixing, ΔG_{mix}, the heat of mixing, ΔH_{mix}, and concentration fluctuations, $S_{cc}(0)$, etc., of symmetric alloys are symmetric about the concentration $c=\frac{1}{2}$, while for asymmetric, or compound forming alloys, this property does not hold, reflecting the existence of chemical complexes in the molten state. Many of these

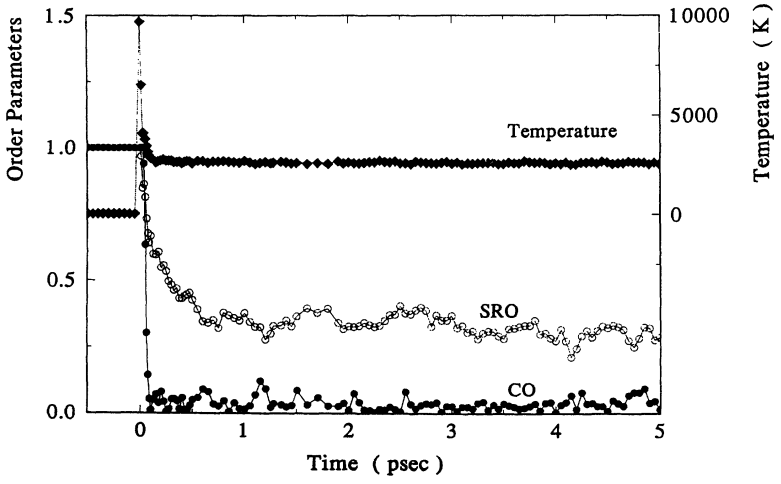

FIG. 1. The time evolution of the short-range order parameter, the crystalline order parameter and the temperature in Ni_3Al as a response to a heat pulse at $t=0$ with $T_0=10\,000$ K initial temperature.

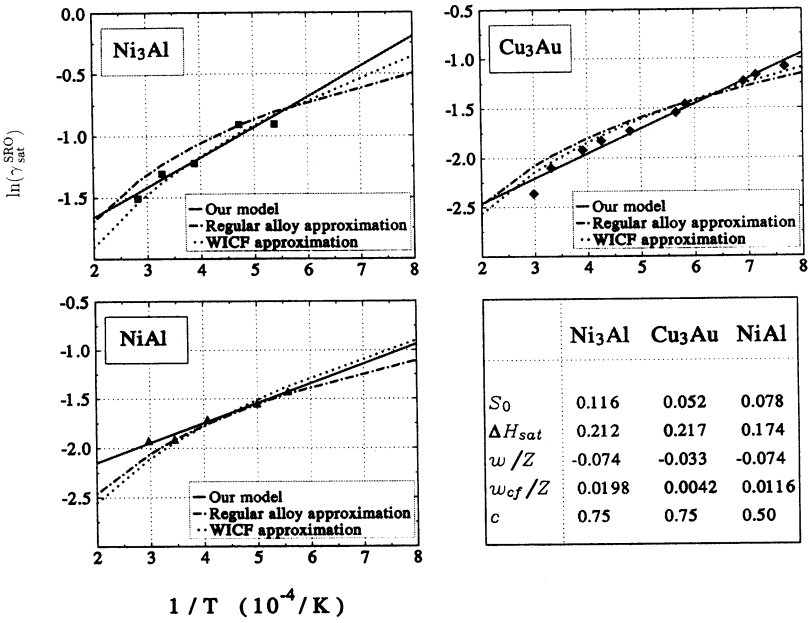

	Ni_3Al	Cu_3Au	NiAl
S_0	0.116	0.052	0.078
ΔH_{sat}	0.212	0.217	0.174
w/Z	-0.074	-0.033	-0.074
w_{cf}/Z	0.0198	0.0042	0.0116
c	0.75	0.75	0.50

FIG. 2. The temperature dependence of the saturation value of the short-range order parameter γ_{sat}^{SRO} in Ni_3Al, Cu_3Au, and NiAl. Symbols are the results of molecular-dynamics (MD) simulations, lines are based on the theoretical assumption.

alloys give metallic glasses in the condensed phase. The theories used to describe them are based on the assumption that there exist in the melt a privileged group of atoms that influence the short-range order, A_mB_n, where A and B denotes the two chemical species, and m and n are small integers related to the concentrations of the stoichiometric solid-state compounds. We base our analysis in the work by Singh,[16] which, in turns, uses developments made by Bhatia and Thornton[17]. Using a quasilattice theory for regular alloys based on a parametrization describing pair interactions, Singh arrives at the following results:

$$\alpha_1=\frac{\beta-1}{\beta+1},\quad \beta=\sqrt{1+4c(1-c)(\eta^2-1)}\,,$$
$$\eta=\exp\left[\frac{w}{Zk_BT}\right] \tag{8}$$

where Z is the coordination number and $w=Z[\varepsilon_{AB}-\frac{1}{2}(\varepsilon_{AA}+\varepsilon_{BB})]$ is the interchange energy with ε_{AA}, ε_{AB}, and ε_{BB} the energies of an AA, AB, or BB pair of atoms. Here we note that in [16–19] the coordination number (Z) is a temperature independent parameter. Our simulations show that the coordination number defined above has a slight temperature dependence, which will be described in details in Sec. III B 3.

According to the weakly interacting compound forming model of Bhatia and Singh[18] based on the quasichemical approximation, in which they assumed (i) the existence of chemical complexes in the liquid phase and (ii) a weak tendency to form complexes, one arrives at another approximation for α_1:

$$\alpha_1=\frac{x}{1+x},\quad x=\frac{2c(1-c)}{Zk_BT}(w+w_{cf}) \tag{9}$$

where w_{cf} is a concentration-dependent contribution with some additional parameters.

It is easy to show that there is a straightforward conversion between α_1 and SRO defined in Eq. (5) and in Eq. (6); therefore they have the same physical meaning. This conversion factor is $(c-1)/c$, which results in a multiplicative factor $-1/3$ in the case of the $L1_2$ alloys and -1 for NiAl in our SRO definition. Because of this, our results can be compared with the predictions of the regular and the weakly interacting compound forming alloy approximations (further noted as WICF), see Fig. 2. Here we note for the clarity, that our model has two free parameters, S_0 and ΔH_{sat}, while the regular alloy and the WICF approximations have only one, the interchange energy (w). There is also a second parameter in these two latter models, namely, the concentration of one species (c), but it cannot be chosen freely because it defines the system of interest. We summarize the values of the parameters in the table of Fig. 2.

The interchange energy (w) in the theory of binary liquids has an important meaning: it indicates the tendency of unlike-atom pair forming if $w<0$, perfect disordering of atoms in the liquid if $w=0$ and like-atom pairing forming if $w>0$. Foiles[13] has developed a pair-potential approximation to the embedded atom model. Generalizing it to the two-component systems, we can compare the corresponding interchange energies of the three theories, see Fig. 3.

In Fig. 3 one can see, that all of the three theories shows the same tendency for the three examined alloys: (i) the interchange energies are negative indicating unlike-atom pair preference in the liquid phase (ii) Cu_3Au has the lowest and Ni_3Al has the highest absolute value showing that Cu_3Au is the most disordered alloy and that Ni_3Al has the strongest tendency to form unlike-atom pairs. The interchange energy of NiAl lies between the values of the two $L1_2$ alloys. This latter observation contradicts the outcome of the ordering energies (see Table I) that would indicate a higher-ordering enthalpy in NiAl

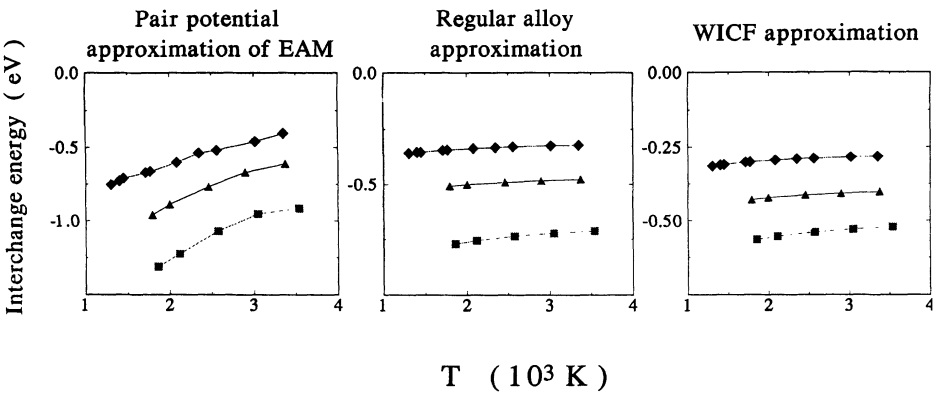

FIG. 3. The interchange energies in Ni_3Al (boxes), Cu_3Au (diamonds) and NiAl (triangles), based on our assumption, on the regular alloy approximation and on the WICF approximation.

than in Ni_3Al, so it can be concluded that the ordering energy calculated from simulation results at 0 K cannot explain the ordering level of the liquid phase.

The slight temperature dependence can be seen in Figs. 3(b) and 3(c) for the regular alloy and the WICF approximations, respectively, and it originates from the temperature dependence of the coordination number used by us. The stronger dependence of w in our model comes from an additional contribution, namely, from temperature dependence of the bond lengths and the bond-energy because of the thermal expansion.

2. *The temperature dependence of the relaxation time of SRO*

When the system melts because of a sudden heat pulse, the disordering process takes some time to bring the system to the equilibrium liquid state. This transient is characterized by a relaxation time. In order to determine the behavior of the relaxation time of the short-range order parameter as a function of the temperature, five simulation events were performed in each intermetallic with the same energy and boundary conditions and with the same initial temperatures mentioned in the introduction part of this section. The relaxation time τ values were calculated from the negative inverse of a linear fitting of the logarithm of the SRO values in the [0.015,0.10] time interval (containing approximately 80 points). The same temperature dependence was assumed as in the case of the saturation value; see Eq. (4):

$$\tau(T)=\tau_0 \exp\left[\frac{\Delta H_\tau}{kT}\right], \tag{10}$$

where the two parameters τ_0 and ΔH_τ are determined by fitting a linear equation for the $\tau-T$ set of points. The simulated points and the theoretical curves fitted to these points are shown in Fig. 4, the calculated parameters of Eq. (10) are in Table II. It shows that (i) NiAl has the fastest response in the whole of the examined temperature range and (ii) at temperatures above about 1600-K Ni_3Al disorders faster than Cu_3Au, while below this temperature the sequence is reversed.

3. *The temperature dependence of the coordination number*

In calculating the coordination number (Z) defined in Sec. III B 1, it was found that it is a function of the temperature. From the definition of Z, the first-nearest

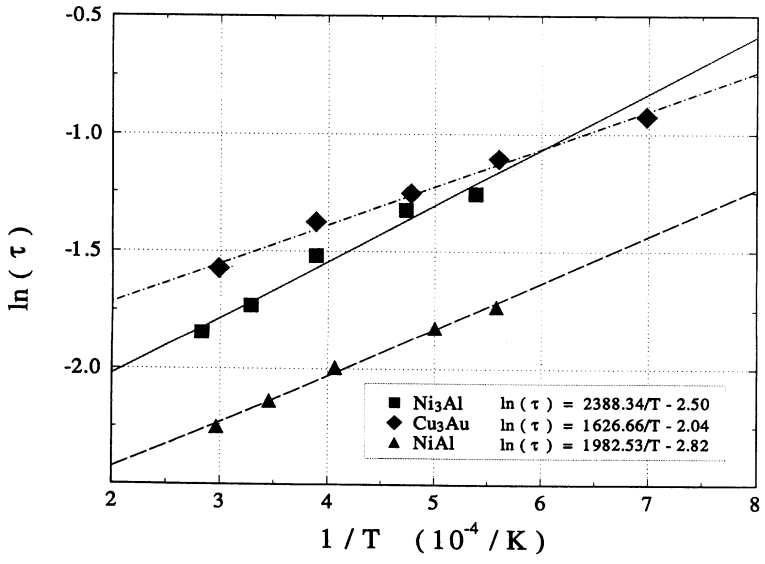

FIG. 4. Temperature dependence of the relaxation time of the short-range order parameter in Ni_3Al, Cu_3Au, and NiAl. Symbols are the results of MD simulations; lines are based on the theoretical assumption.

TABLE II. The calculated parameters for the temperature dependence of the relaxation time of SRO.

	Ni_3Al	Cu_3Au	NiAl
ΔH_τ (eV)	0.206	0.140	0.171
τ_0 (psec)	0.082	0.131	0.059

neighbors are in a range of distances and a cutoff is used that separates them from the farther neighbors. The radial distribution functions have been calculated and as can be seen on Fig. 5 for Ni_3Al, the positioning and the integration of the first peak in the distribution does not provide more precise information than that obtained from the definition used by us. In Figs. 6(a), 6(b), and 6(c) we present the simulation results for the temperature dependence of the coordination number for Ni_3Al, Cu_3Au, and NiAl, respectively. The examined two theoretical approximation (a linear and an exponential dependence with the inverse of the temperature) shows no significant differences; therefore we plot the fitted curves only for the linear approximation.

If we examine in details the coordination number in the two sublattices we find that (i) in the $L1_2$ alloys there is no significant difference in the coordination number, i.e., $t1$ and $t2$ atoms have closely the same number of nearest neighbors regardless of the type of the neighbors, see Figs. 6(d) and 6(e), (ii) the curves cross each other at

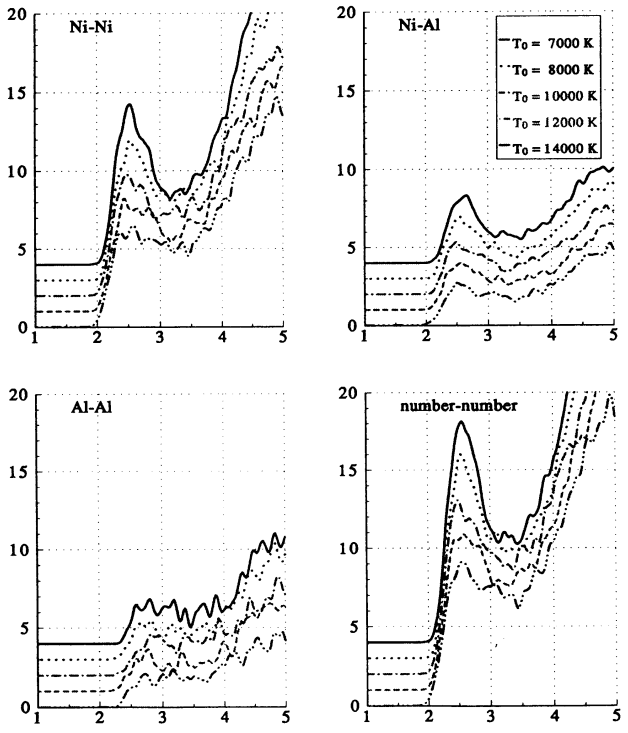

FIG. 5. Radial distribution functions for Ni_3Al.

~2550 K in the case of Ni_3Al and at ~1970 K in Cu_3Au, and (iii) in the case of NiAl the coordination number has higher values in the Ni sublattice, indicating that Ni (type-1) atoms have more nearest neighbors as an average than the Al (type-2) atoms; see Fig. 6(f). It is also useful to examine the discrepancy of the like and unlike nearest-neighbor numbers from the ideal mixture and ideal solid values. These quantities show a very similar behavior to the behavior of the coordination number; see Fig. 7: (i) again no large difference between the two sublattices in the $L1_2$ intermetallics and (ii) in NiAl the discrepancy from the ideal mixture values is larger in the Al sublattice than in the Ni sublattice, while it is just the opposite if we compare the absolute values of the discrepancies from the ideal solid. In other words, in NiAl, the average coordination number in the type-1 sublattice is closer to coordination number values of the ideal mixture, while the type-2 sublattice rather looks like an ideal solid. It is interesting to notice that in the $L1_2$ alloys the curves cross each other at exactly the temperature where the coordination numbers in the sublattices cross each other. The positive values in Figs. 7(d), 7(e), and 7(f) indicate, that in the liquid phase of these alloys an atom has more unlike-type nearest neighbors than in the ideal mixture, as an average. This is a sort of verification of the negative values of interchange energy that also suggest the preference of the unlike-atom pair formation. Summarizing the discrepancy data calculated in the sublattices we get the total discrepancies from the ideal mixture and ideal solid. These quantities can be seen in Fig. 8. Comparing the values it can be found that (i) Cu_3Au resembles the best the ideal mixture, (ii) the disordering level of NiAl is higher than the disordering level of Cu_3Au, but the difference is small, and (iii) Ni_3Al is the most ordered liquid among these three intermetallics.

4. *The mean-squared displacements*

To follow the development of the disordering process with the atomic migration, we calculate the mean squared displacements (MSQD's) at 5 psec in the $L1_2$ alloys and at 3 psec in NiAl for both constituent species. Previous cascade simulations in Ni_3Al and Cu_3Au (Refs. 7 and 8) show that the mobilities of the majority and minority species are identical, indicating no relationship between the vacancy migration in the solid and the diffusion mechanisms. Recent simulation of 5-keV Ni PKA cascade in NiAl results in about 15% higher values for the mean square displacements of the Ni atoms. Since this difference in the number of the displaced atoms is only 5% we can conclude that the Ni atoms move farther from their original position than the Al atoms on the average.

In the dynamical melting simulations we found that there is no important difference between the sublattices in all of the three alloys and the values for the type-2 atoms are always a little lower than the values of the type-1 species. The magnitude of the MSQD's normalized to number of displaced atoms at a given temperature are also close together for the different alloys. It means that we cannot explain the different behavior of the Ni and

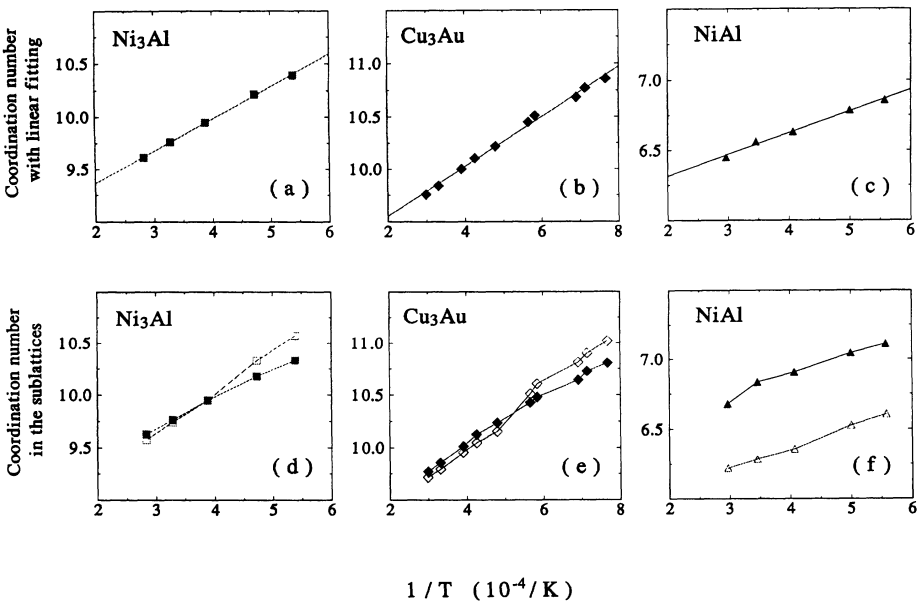

FIG. 6. The temperature dependence of the total coordination number calculated from the sublattice coordination number [shown in (d)–(f)] by weighting respect to the number of atoms of the sublattices. In (d)–(f) open symbols mean type-I (Ni or Cu) sublattice values; full symbols were calculated in the type-2 (Al or Au) sublattice. In (a)–(c) symbols are MD simulation results, lines are the fitted curves based on the linear dependence assumption.

the Al sublattices in NiAl with the amount of atomic motion so we have to suppose that a large number of Al atoms simply goes to the "wrong" place from the viewpoint of the ideal mixture. It may be the indication of the compound forming tendency in the liquid phase of the Ni-Al system, namely, that the preferred phase is not the perfectly disordered mixture but some kind of complex (or more probably complexes) between the (1,1) and (3,1) composition.

IV. THEORETICAL MODEL OF SRO

To explain the behavior of the short-range order parameter observed in the locally melted zones of the cascade simulations, reported for Ni_3Al and Cu_3Au in Refs. 7, 8, we assume a standard relaxation time approximation for the time evolution of SRO:

$$\frac{dS(t)}{dt}=-\frac{S(t)-S_{\text{sat}}}{\tau}\ , \tag{11}$$

where $S_{\text{sat}}=S_{\text{sat}}(T(t))$ and $\tau=\tau(T(t))$ are obtained from (4) and (10). We assume a Gaussian temperature distribution as an approximation to the temperature distribution in the core of collisional cascades,

$$T(r,t)=\frac{T_0}{[\sqrt{2\pi}(\sigma_0+\sqrt{Dt}\,)]^3}\exp\left[\frac{-r^2}{2(\sigma_0+\sqrt{Dt}\,)^2}\right]$$

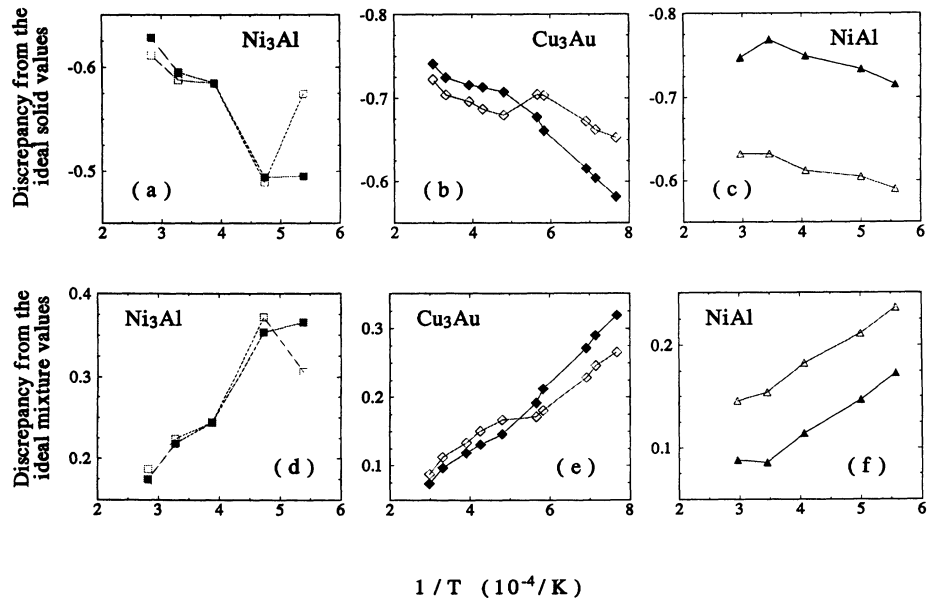

FIG. 7. Discrepancy of the calculated coordination number from the ideal solid (a)–(c) and ideal mixture values (d)–(f).

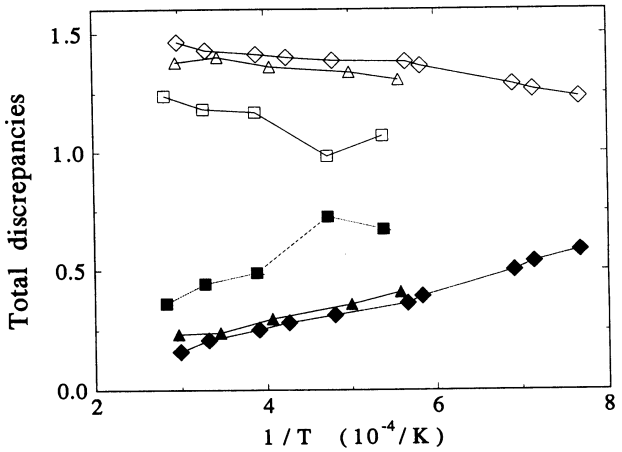

FIG. 8. Total discrepancies of the coordination number in Ni_3Al, Cu_3Au, and NiAl.

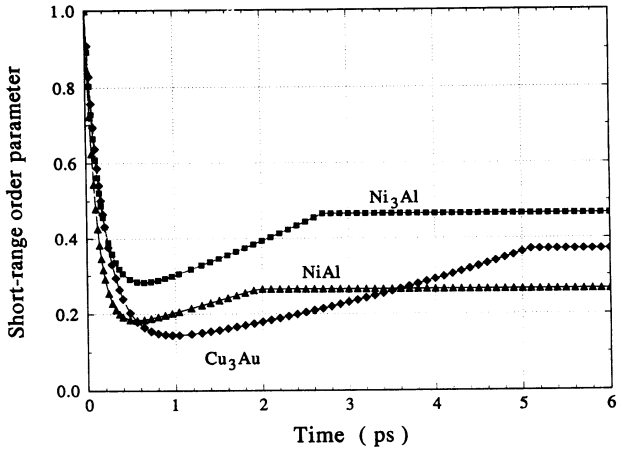

FIG. 9. The time evolution of the short-range order parameter predicted by our model for Ni_3Al, Cu_3Au, and NiAl.

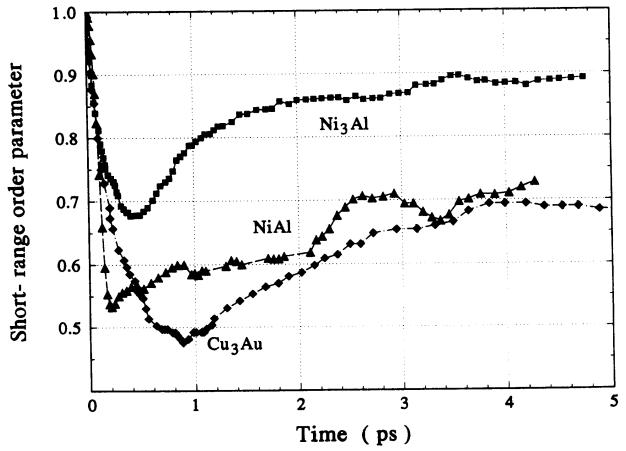

FIG. 10. The time evolution of short-range order parameter in 5-keV cascades in Ni_3Al, Cu_3Au, and NiAl.

with three free parameters: σ_0, D, and T_0. The numerical solution of (11) for reasonable values for 5-keV cascades, namely, $\sigma_0=0.4713$ Å, $D=0.015$ Å^2/psec, and $T_0=8000$ K Å^3 is shown in Fig. 9. Comparing this figure with Fig. 10, which is the result of the cascade simulations (see Refs. 7 and 8 for the $L1_2$ alloys; the NiAl result is unpublished), it can be seen that our analytic description of the chemical short-range order parameter based on the kinetics of the melting transition can describe the main features of time evolution of SRO resulting from high-energy-displacement cascade as simulated in these intermetallics.

V. CONCLUSION

The liquid phase of three intermetallic binary alloys, Ni_3Al, Cu_3Au, and NiAl have been simulated with molecular-dynamics techniques in order to investigate the kinetics of the ordering processes appearing in the core of the collision cascades of these compounds. We give a theoretical model for the time evolution of the short-range order parameter based on a standard relaxation-time approximation. The elementary static point-defect formation enthalpies and formation volumes are also presented, as well as some thermodynamic data predicted by the embedded atom potentials. Our results show the following.

The time sequence in which the most disordered state is reached is correctly predicted, i.e., NiAl is the fastest and Cu_3Au is the slowest alloy.

The predictions that Ni_3Al has the highest degree of order at the end of the cascade, and that the disordered levels of Cu_3Au and NiAl are close together, is also in agreement with the cascade simulation results.

There is a small discrepancy in the final values of SRO, which is probably due to the assumption of identical initial temperature distribution in the three systems.

Our simple approximation represented by Eq. (11) gives a better fit to the simulated points than the regular alloy and the weakly interacting compound forming approximation.

All of the three models (regular alloy and WICF approximation and our model) give the same sequence for the interchange energy in the whole examined temperature range, which indicates that Cu_3Au is the most disordered and Ni_3Al is the most ordered alloy, while the disordering level of NiAl lies between the two $L1_2$ alloys. The negative value shows unlike-atom pair preference in the liquid phase of these three intermetallics.

We found that the temperature dependence of the coordination number can be described fairly well if we assume an exponential dependence with the inverse of the temperature.

We observe an interesting behavior in the energetics of the several self-interstitials, namely, sorting the intersti-

tials by increasing formation enthalpy two alternatives seems to be have occurred: (i) the chemical nature of the interstitial determines which are those energetically preferred, and (ii) the location of the defect is more important than its type to determine the enthalpy. The two $L1_2$ structures can be classified in the second group, while in NiAl the lowest formation enthalpies always belong to the Ni interstitials regardless of the layer.

ACKNOWLEDGMENT

This work was partially supported by a grant from the Swiss National Science Foundation.

[1]H. C. Liu and T. E. Mitchell, Acta Metall. **31**, 863 (1983).
[2]J. Eridon, G. S. Was, and L. Rehn, J. Mater. Res. **3**, 626 (1988).
[3]L. S. Hung, M. Nastasi, J. Gyulai, and J. W. Mayer, Appl. Phys. Lett. **42**, 672 (1983).
[4]J. P. Rivière, C. Jaouen, and J. Delafond, Mater. Sci. Forum **15-18**, 1111 (1987).
[5]C. Jaouen, J. P. Rivière, and J. Delafond, Nucl. Instrum. Methods B **19/20**, 549 (1987).
[6]L. Thomé, C. Jaouen, J. P. Rivière, and J. Delafond, Nucl. Instrum. Methods B **19/20**, 554 (1987).
[7]T. Diaz de la Rubia, A. Caro, and M. Spaczér, Phys. Rev. B **47**, 11 483 (1993).
[8]T. Diaz de la Rubia, A. Caro, M. Spaczér, G. A. Janaway, M. W. Guinan, and M. Victoria, Nucl. Instrum. Methods B **80/81**, 86 (1983).
[9]M. Parrinello and A. Rahman, Phys. Rev. Lett. **45**, 1196 (1970).
[10]M. Parrinello and A. Rahman, J. Appl. Phys. **52**, 7182 (1981).
[11]S. M. Foiles, M. I. Baskes, and M. S. Daw, Phys. Rev. B **33**, 7983 (1986).
[12]S. M. Foiles and M. S. Daw, J. Mater. Res. **2**, 5 (1987).
[13]S. M. Foiles, Phys. Rev. B **32**, 3409 (1985).
[14]A. Caro, M. Victoria, and R. S. Averback, J. Mater. Res. **5**, 1409 (1990).
[15]F. Gao and D. J. Bacon, Philos. Mag. A **67**, 275 (1993).
[16]R. N. Singh, Can. J. Phys. **65**, 309 (1987).
[17]A. B. Bhatia and D. E. Thornton, Phys. Rev. B **2**, 3004 (1970).
[18]A. B. Bhatia and R. N. Singh, Phys. Chem. Liq. **11**, 343 (1982).
[19]A. B. Bhatia and R. N. Singh, Phys. Chem. Liq. **11**, 285 (1982).